Applied Catalysis B: Environmental 146 (2014) 221–226

Contents lists available at ScienceDirect

Applied Catalysis B: Environmental

journal homepage: www.elsevier.com/locate/apcatb

Aqueous phase reforming of ethanol and acetic acid over TiO_2 supported Ru catalysts

Toshiaki Nozawa, Yuichi Mizukoshi, Akihiro Yoshida, Shuichi Naito*

Department of Material and Life Chemistry, Kanagawa University, 3-27-1 Rokkakubashi, Yokohama, Kanagawa-ku 221-8686, Japan

ARTICLE INFO

Article history:
Received 29 October 2012
Received in revised form 27 April 2013
Accepted 18 June 2013
Available online 27 June 2013

Keywords:
Aqueous phase reforming
Ethanol
Acetic acid
Acetaldehyde
Ruthenium

ABSTRACT

This study examined the dependence of Ru particle sizes upon the activity and selectivity for aqueous phase reforming reactions of ethanol and acetic acid over Ru/TiO_2 at 473 K. For ethanol, irrespective of the Ru particle size, the 1:1 ratio of CH_4 and CO_2 was formed at the initial stage, indicating the absence of complete reforming with water. At the later stage, unfavorable methanation of CO_2 by H_2 was observed over larger Ru particle catalysts. That methanation was suppressed completely over smaller Ru particle catalysts. In the case of acetic acid reforming over smaller Ru particle catalysts, a 2:1 ratio of H_2 and CO_2 was formed constantly, indicating the operation of complete reforming reaction with water. Positively charged small Ru particles were responsible for the efficient activation of acetic acid and water to form H_2 and CO_2 selectively.

© 2013 Elsevier B.V. All rights reserved.

1. Introduction

Hydrogen production from bio-renewable sources is regarded as a promising means to minimize environmental problems associated with fossil fuel combustion [1,2]. Catalytic reforming of ethanol appears to be an excellent strategy to obtain hydrogen. It has two methods: steam reforming (SR) [3–5] and aqueous phase reforming (APR) [6–9]. During ethanol steam reforming processing, many competing reactions take place, producing undesirable light hydrocarbons as well as CO, which requires a lower-temperature water-gas shift reaction. In addition, most catalysts used for ethanol steam reforming entail problems of severe deactivation by material degradation and carbon deposition at higher temperatures. Compared with usual steam reforming reaction, the advantages of liquid phase reforming are the possibility of producing more compact and simple reaction equipment and the obviation of evaporation energy of aqueous solutions. In spite of its importance, few studies have examined liquid-phase reforming from the viewpoint of heterogeneous catalysis, except for an anode reaction in direct methanol fuel cells (DMFCs) [10,11].

Recently, Dumesic et al. reported the liquid phase reaction of methanol, ethylene glycol and other oxygenates with water over supported Pt and Ni catalysts [12–14]. The mechanism of H_2 production from ethylene glycol, described by Shabaker et al. [15,16], involved the cleavages of C—C and C—H bonds to form adsorbed CO followed by water-gas shift to H_2 and CO_2 formation. Consequently, a good catalyst for APR process must be active in the cleavage of C—C bonds and water-gas shift reaction, but it must inhibit the cleavage of C—O bond and methanation reactions. Generation of H_2 and CO_2 by liquid phase reforming at low temperatures, however, is accompanied by selectivity challenges because the reaction of H_2 and CO or CO_2 to form alkanes is highly favorable at these low temperatures. The H_2 selectivity is dependent on the type of metals, the nature of the support, the feed reactant molecules, and the reaction conditions [17].

It has been generally accepted that alcohols such as methanol, ethylene glycol, and glycerol, where the C—H bond of each carbon atom is activated by adjacent OH groups, might be converted selectively to H_2 and CO_2 [15,18–21]. However, for ethanol, it is rather difficult to obtain H_2 and CO_2 selectively as complete reforming products because of the non-activated methyl group, which is easily transformed to CH_4 [22–24]. Accordingly, in ordinary cases, we will obtain a 1:1 ratio of CH_4 and CO_2 together with acetic acid. In addition, that formed CO or CO_2 is transformed into CH_4 through a methanation reaction, which results in an excess CH_4 compared to CO_2. It is apparently quite difficult to reform CH_4 under usual APR conditions. However, a possibility of reforming acetic acid in SR as well as APR reactions exists at lower temperatures [25–30].

Recently, we studied aqueous phase reforming of ethanol over various TiO_2 supported precious metal catalysts [31]. Their activity and selectivity differ depending on the kind of metal with the following activity order: Ru > Rh > Pt > Ir > Pd. For Pt and Ir, a large amount of acetic acid was formed by the hydration of acetaldehyde with smaller amounts of CO_2 and CH_4 (1:1 ratio), indicating

* Corresponding author. Tel.: +81 45 481 5661.
E-mail address: naitos01@kanagawa-u.ac.jp (S. Naito).

0926-3373/$ – see front matter © 2013 Elsevier B.V. All rights reserved.
http://dx.doi.org/10.1016/j.apcatb.2013.06.017

Table 1
Characterization of employed Ru/TiO_2 catalysts.

Ru/TiO_2 loading amt. (wt%)	Fresh catalysts					Used catalysts	
	Amt. of CO(a) (mL/g)	Disp. (%)	Particle size (nm)		$Ru^{\delta+}/Ru^0$	Amt. of CO(a) (mL/g)	Disp. (%)
			CO(a)	TEM	XPS		
5.0	12.1	24.6	5.4	2.3	0.09	9.51	19.3
2.0	9.47	48.8	2.7	1.2	0.11	7.01	36.1
1.0	9.36	91.3	1.4	–	–	6.79	66.2
0.5	5.24	119.7[a]	1.1	–	0.19	3.85	88.0

[a] Probably because of the presence of a small amount of $Ru(CO)_x$ ($x > 1$) species.

the absence of reforming process. However, for Rh, major products were CH_4 and CO_2 with a small amount of liquid phase products and excess CH_4 formed afterward, indicating the operation of an unfavorable methanation reaction.

This study specifically examined Ru metal because it shows the highest activity but the lowest selectivity among the metals. Selectivity-controlling factors in aqueous ethanol, acetaldehyde, and acetic acid reforming reactions were investigated by changing the Ru particle size. Results showed that small, positively charged Ru particle catalysts can suppress unfavorable methanation reactions and realize a complete reforming reaction of acetic acid to form H_2 and CO_2.

2. Experimental

2.1. Preparation of catalysts and reaction procedures

Supported Ru catalysts (0.5, 1.0, 2.0, and 5 wt%) were prepared using a conventional impregnation method employing $RuCl_3 \cdot xH_2O$ as a precursor and TiO_2 (P-25, surface area = 50 m^2/g; Nippon Aerosil Co. Ltd.) as a support. The impregnated samples were dried overnight at 373 K, and were reduced by 1 atm hydrogen flow at 623 K for 5 h. The reduced catalyst (0.5 g) was put into a stainless steel autoclave (400 ml) and was reduced again by 5 vol% H_2/N_2 flow at 623 K for 1 h. After purging hydrogen using pure N_2, 80 ml of degassed aqueous solution of reactants (EtOH; 10 vol%, AcOH and AcH; 1 vol%) was introduced into the reactor under nitrogen atmosphere. The reforming reaction was conducted in a batch mode, which was connected to an online TCD gas chromatograph to analyze the gas phase products during the reaction (molecular sieve 13× column). After quick heating (about 30 min), the reaction was started at 473 K under 2.5–3.0 MPa pressure. During the reaction, the liquid phase content of the autoclave was stirred vigorously by a magnetic stirrer. A small part of the liquid phase products was sampled using an online sampling tube (1 ml) and analyzed using an FID gas chromatograph (CP PoraBond Q column).

2.2. Characterization of catalysts

A transmission electron microscope (JEM-2010; JEOL) with acceleration voltage of 200 kV and LaB_6 cathode was applied to observe images of the supported catalysts. Samples were prepared by suspending the catalyst powder ultrasonically in methanol and by depositing a drop of the suspension on a standard copper grid covered with carbon monolayer film. X-ray photoelectron spectroscopy (JPS-9010; JEOL) with a Mg Kα X-ray source (10 kV, 10 mA) was applied for the analysis of the chemical states of the catalysts. The catalyst was pressed into a 20 mm diameter disk and was pretreated by H_2 at 623 K. Then the disk was mounted on the sample holder of the XPS preparation chamber, after which it was reduced again by H_2 at 623 K and transferred to the analysis chamber without exposure to air. The observed binding energy was calibrated using a C_{1s} transition peak at 284.5 eV.

The amounts of CO adsorption were measured using a static volumetric adsorption apparatus (Omnisorp100CX; Beckmann Coulter Inc.) at room temperature. Before the measurement, a fresh catalyst was reduced by H_2 at 623 K for 2 h. To investigate the influence of metal sintering during reforming reaction at 473 K, the used catalyst was separated by filtration and dried. The obtained sample was provided for CO adsorption measurements. The metal dispersion (D (%): percentage of metal atoms exposed to the surface) on the support was evaluated from the amount of chemisorbed CO by assuming the stoichiometry of CO(a)/M = 1.

Fourier transform infrared spectroscopy (FT-IR) measurements were conducted using a self-support catalyst disk mounted in a transmission cell and a FT-IR spectrometer (FT-IR6100; Jasco Corp.) equipped with a closed gas circulation system. Similar pretreatment as the reaction procedure was conducted before CO adsorption measurements.

3. Results and discussion

3.1. Catalysts characterization

The Ru particle sizes were controlled by changing the loading amounts of metal precursors in the impregnation procedure. Table 1 presents the amounts of adsorbed CO at room temperature over fresh and used catalysts, together with the estimated particle sizes by assuming the hemisphere shape of Ru metal on the support with the adsorption stoichiometry of CO/Ru = 1. The dispersion of fresh catalysts exhibited an almost linear relation with the loading amounts. After 10 h ethanol reforming at 473 K, the dispersion was decreased to 80–70% of the fresh catalyst, probably because of the sintering of Ru metal. The data are summarized at the last column of Table 1, which are the values used for TOF estimation.

Fig. 1 presents TEM images of freshly reduced 5 and 2 wt% catalysts. The average particle diameters observed were 2.32 and 1.52 nm respectively, of which the values were nearly half of the estimated values from CO adsorption, probably because of the SMSI effect of Ru/TiO_2 catalysts [32]. For the 1 and 0.5 wt% catalysts, it was impossible to obtain clear TEM images because of the interference of dark images of TiO_2 particles. Fig. 2 shows the XPS spectra of Ru3d transition of Ru/TiO_2 catalyst taken after the in situ reduction by H_2 at 623 K. Because the $Ru3d_{3/2}$ peak was overlapped completely with the C1s peak, it was not so easy to determine the binding energies precisely. However, by the deconvolution of Ru^0 (B.E. = 279.8 eV), $Ru^{\delta+}$ (281.2 eV) and Ru^{3+} (282.4 eV) peaks (spec. surf. software; JEOL), we were able to estimate the relative intensity ratios of zero-valent Ru and positively charged Ru species ($Ru^{\delta+} + Ru^{3+}$) on 5, 2 and 0.5 wt% catalysts, as presented in Table 1. These results reflect that most of the surface Ru species in smaller metal particles are positively charged, probably through the electronic interaction with the support.

Fig. 3(A) represents the FT-IR spectra of adsorbed CO at room temperature over various amounts of Ru loaded catalysts. For the 5 wt% catalysts, three characteristic bands were observed at 2036–2043, 2087, and 2149 cm^{-1}. The low frequency band can be

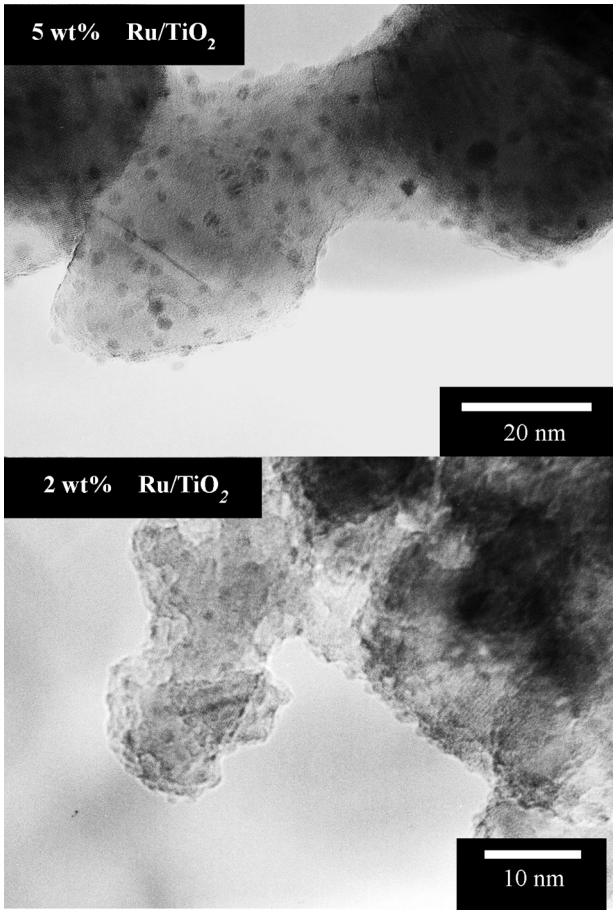

Fig. 1. TEM images of 5 and 2 wt% Ru/TiO_2.

assigned to linearly adsorbed CO on top of the zero valence Ru metal with larger particle sizes, which many research groups have confirmed [33–35]. However, some controversy persists about the assignment of medium-frequency and high-frequency bands in the literature. For Ru/SiO_2 [33] and Ru/Al_2O_3 [34] catalysts, these two bands were assigned to the symmetric and asymmetric stretches of two CO molecules bonded to a single oxidized Ru sites (geminal CO species). To clarify this point, the temperature programmed desorption (TPD) of adsorbed CO over 5 wt% Ru/TiO_2 was followed as presented in Fig. 3(B). At higher temperatures, the high frequency band disappeared much faster than the medium frequency one, indicating that these two bands belong to different sites of two kinds of oxidized Ru species, similar to the case of Ru/NaY Zeolite [35]. In Fig. 3(A), as the particle size became smaller, the relative intensity of the low-frequency CO(a) peak on larger Ru particle sites become smaller than the high-frequency and medium-frequency CO(a) peaks on positively charged smaller Ru particles, which is consistent with the XPS results presented in Table 1.

3.2. Aqueous phase reforming of ethanol over Ru/TiO_2

Fig. 4 shows the time courses of the aqueous phase reforming of ethanol over (A) 5 and (B) 0.5 wt% Ru/TiO_2 catalysts at 473 K. In both cases, H_2, CH_4, and CO_2 were the major products in the gas phase with a small amount of acetaldehyde (AcH) and acetic acid (AcOH) in the liquid phase. Because no CO was detected during the reaction, the water-gas shift reaction to form CO_2 is expected to occur very rapidly under aqueous phase reaction conditions. Over 5 wt% catalyst, the rates of H_2 and CO_2 formation decreased considerably after 200 min, although the amount of CH_4 increased

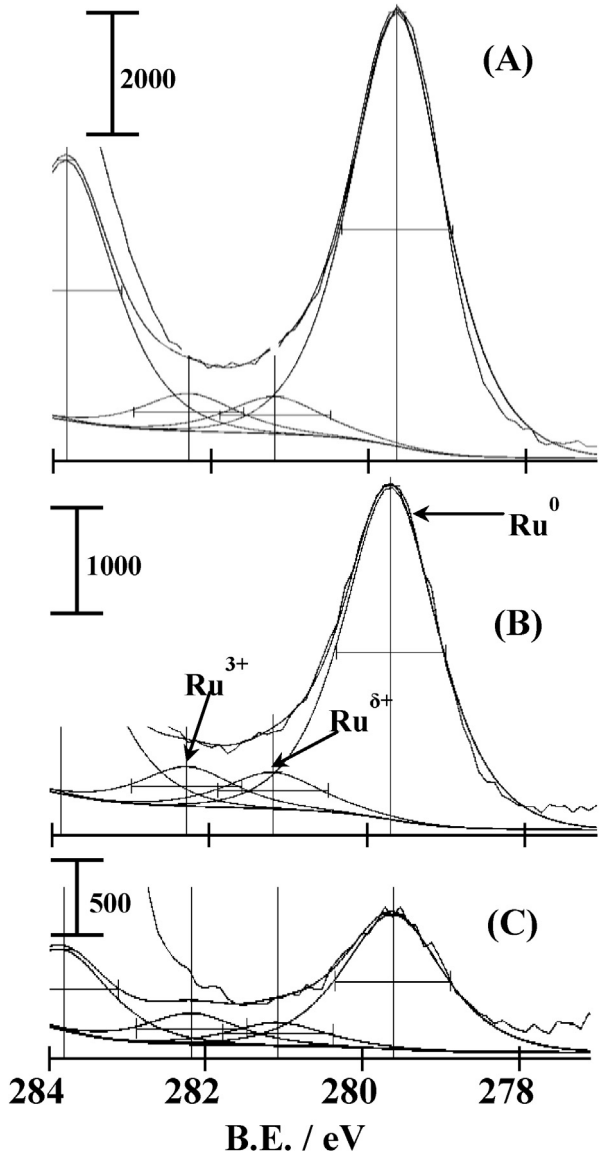

Fig. 2. XPS spectra of Ru/TiO_2 after in situ reduction by H_2 at 573 K. (A) 5 wt%, (B) 2 wt%, and (C) 0.5 wt%.

continuously. Because Ru metal is an excellent catalyst for CO and CO_2 hydrogenation, this might be explained using the occurrence of successive methanation of CO_2 with H_2. However, over 0.5 wt% catalyst main product was H_2, even after 10 h with smaller amount of CH_4 and CO_2 (1:1 ratio). This result strongly suggests the prevention of undesirable methanation over lower metal loading catalysts.

The first step of aqueous ethanol reforming would be the dehydrogenation of ethanol giving acetaldehyde (AcH) ($CH_3CH_2OH \rightarrow CH_3CHO + 1/2H_2$), which goes to two different reaction pathways, (1) decomposition to form CH_4 and CO (reaction path-I; $CH_3CHO \rightarrow CH_4 + CO$, $CO + H_2O \rightarrow CO_2 + H_2$), and (2) hydration to form acetic acid (AcOH) (reaction path-II; $CH_3CHO + H_2O \rightarrow CH_3COOH + H_2$). To clarify the characteristics of the active sites for these two pathways, the turnover frequency (TOF) of the initial rate of product formation was estimated by assuming the values of CO dispersion of used catalysts as the quantities of the reaction sites. Table 2 presents the results of various Ru loading catalysts. Regarding reaction path-I, higher loading Ru/TiO_2 catalysts exhibited larger TOFs of CO_2 and CH_4 formation than lower loading catalysts, whereas, for reaction path-II, the latter catalysts exhibited larger TOFs of AcH and AcOH formation than former

Table 2
Turnover frequency and CO_2/CH_4 ratio of the initial rate of aqueous ethanol reforming reactions over various Ru/TiO_2 catalysts at 473 K.

EtOH (vol%)	Loading amt. (wt%) [Disp. (%)]	Turnover frequency ($\times 10^{-3}$ s^{-1})					CO_2/CH_4	Conv. (%) after 10 h
		H_2	CO_2	CH_4	AcH	AcOH		
10	5.0 [19.3]	23.4	12.9	25.0	0.34	0.00	28.4	28.4
10	2.0 [36.1]	42.7	12.9	17.3	0.21	0.96	0.75	15.8
10	1.0 [66.2]	41.1	10.9	12.5	1.59	1.85	0.87	8.5
10	0.5 [88.0]	56.4	10.0	11.1	3.82	6.99	0.91	6.0
1	0.5 [88.0]	13.9	4.63	4.63	1.09	1.25	1.0	–
1[+AcOH]	0.5 [88.0]	14.4	4.61	4.62	1.14	–	0.99	–

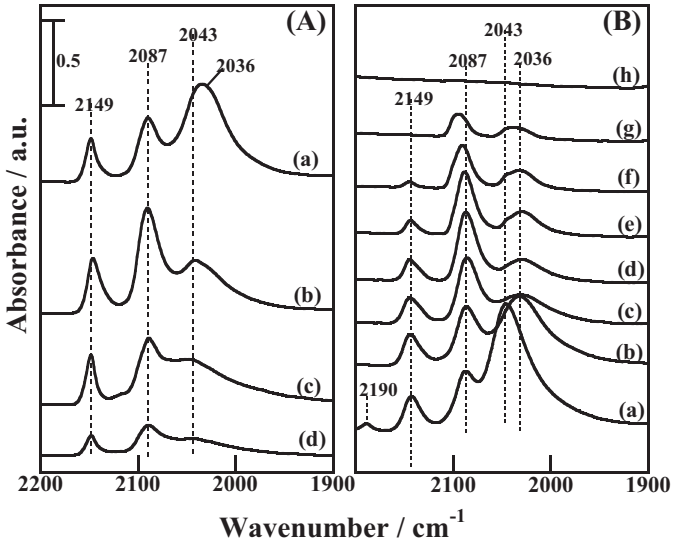

Fig. 3. FT-IR spectra of adsorbed CO at r.t. and its TPD spectra over various Ru/TiO_2. (A) (a) 5 wt%, (b) 2 wt%, (c) 1 wt%, and (d) 0.5 wt%. (B) (a) 10 Torr of CO at r.t., (b) evac. at r.t., (c) TPD at 323 K, (d) at 373 K, (e) 423 K, (f) 473 K, (g) 523 K, and (h) 573 K.

ones, suggesting that these two paths might proceed at different active sites.

3.3. Aqueous phase reforming of acetic acid over Ru/TiO_2

Similar loading amount dependency was observed for the aqueous phase reforming of acetic acid over various Ru/TiO_2 catalysts, where H_2, CO_2, and CH_4 were the major products in the gas phase with a trace amount of liquid phase products. Fig. 5(A) shows the time courses of the reforming reaction over 5 wt% Ru/TiO_2 at 473 K. At the initial stage of the reaction, H_2 and CO_2 were formed quickly, suggesting that the direct reforming of acetic acid with water ($CH_3COOH + 2H_2O \rightarrow 2CO_2 + 4H_2$) was taking place. However, the formation of H_2 almost stopped at 200 min, and the 1:1 ratio of CO_2 and CH_4 was formed continuously thereafter, suggesting the switching of the reaction from reforming to the simple decomposition of AcOH. The time courses were very different in the case of 0.5 wt% Ru/TiO_2, as presented in Fig. 5(B). The formation of H_2 and CO_2 with 2:1 ratio continued constantly for 10 h with a small amount of CH_4, indicating the direct reforming of AcOH with H_2O was taking place. In the cases of 2 and 1 wt% Ru/TiO_2 catalysts, the feature of time courses resembled the mixture of the reactions over 5 and 0.5 wt% catalysts. These situations are presented in Table 3. The TOFs of the initial rate of H_2, CO_2 and CH_4 formation decreased with the increase of Ru dispersion. Over 0.5 wt% catalyst, the ratio of TOF for H_2 and CO_2 is almost 2:1 with a smaller amount of CH_4 formation, indicating the operation of complete AcOH reforming. As the Ru loading amount increased, the H_2/CO_2 ratio became less than 2 with the increase of TOF for CH_4 formation.

3.4. Reaction pathways and the selectivity controlling factors

Fig. 6 shows the time courses of the aqueous phase reforming of acetaldehyde over (A) 5 and (B) 0.5 wt% Ru/TiO_2 at 473 K. Similar results to the previous ethanol reforming were obtained. Over 5 wt% Ru/TiO_2 catalyst, H_2, CH_4 and CO_2 were the main products at the initial stage and the TOF ratio of the initial rates of CO_2 and CH_4 was almost 1, suggesting the operation of reaction path-I. At the later stage, the methanation of CO_2 with H_2 was observed. In the liquid phase, formation of a small amount of AcOH and EtOH was observed, which decreased at the later stage. Over 0.5 wt% Ru/TiO_2 catalyst, H_2, CO_2, and CH_4 were formed with similar initial rates, but

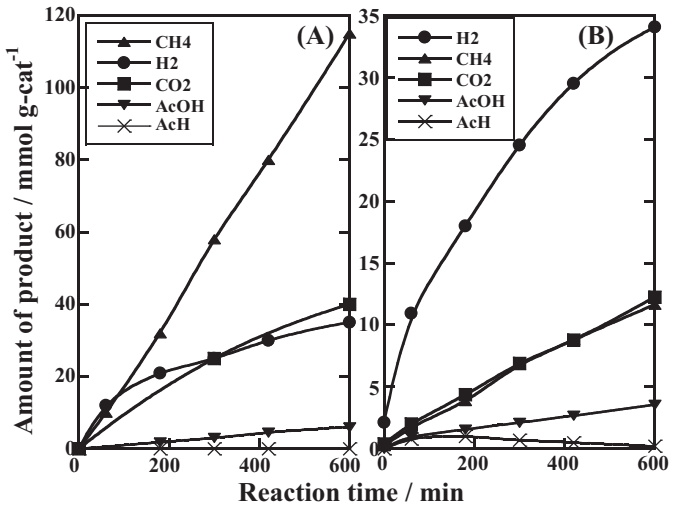

Fig. 4. Time courses of aqueous $EtOH{\cdot}H_2O$ reaction over (A) 5 wt% and (B) 0.5 wt% Ru/TiO_2 at 473 K.

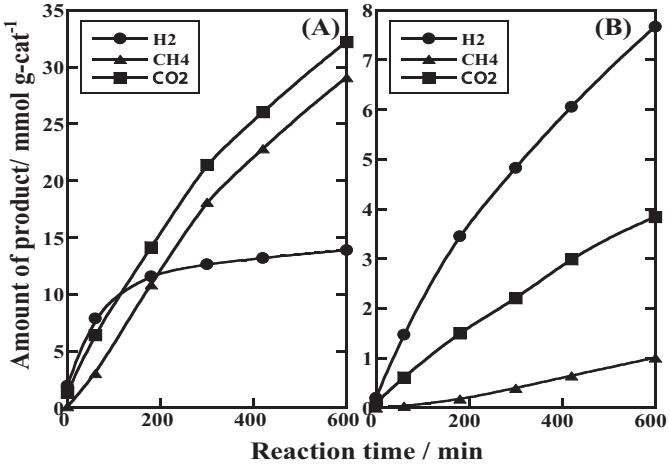

Fig. 5. Time courses of aqueous $AcOH{\cdot}H_2O$ reaction over (A) 5 wt% and (B) 0.5 wt% Ru/TiO_2 at 473 K.

Table 3
Turnover frequency and the CO_2/CH_4 ratio of the initial rate of aqueous acetic acid reforming reactions over various Ru/TiO_2 catalysts at 473 K.

Loading amt. (wt%)	Disp. (%)	Turnover frequency ($\times 10^{-3}$ s^{-1})			CO_2/CH_4	Conv. (%) after 10 h
		H_2	CO_2	CH_4		
5.0	19.3	17.8	14.1	8.5	1.7	99.0
2.0	36.1	16.5	10.5	4.2	2.8	73.7
1.0	66.2	8.2	4.4	0.7	7.4	15.3
0.5	88.0	8.4	3.7	0.3	14.7	8.2

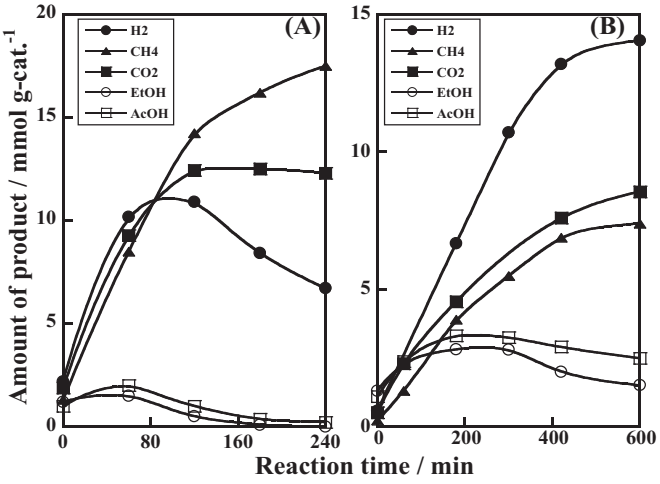

Fig. 6. Time courses of aqueous AcH·H_2O reaction over (A) 5 wt% and (B) 0.5 wt% Ru/TiO_2 at 473 K.

the formation of H_2 continued to increase linearly until acetaldehyde was consumed, and the TOF ratio of CO_2 and CH_4 was about 1.5, indicating the operation of reforming reaction to form CO_2 and H_2. In the liquid phase, comparable amount of AcOH to that of the gas phase was observed, together with the lesser amount of EtOH, with TOF that is larger in smaller Ru metal than larger ones. At the later stage of the reaction, the amount of formed acetic acid and ethanol decreased, indicating the existence of successive irreversible reaction step.

Fig. 7 shows the reaction scheme of aqueous phase EtOH, AcH and AcOH reforming reactions proposed in this study. When we started from EtOH, its dehydrogenation gave AcH, which went to two different reaction pathways, (1) decomposition to form CH_4 and CO followed by the water gas shift to form H_2 and CO_2, (2) hydration to form AcOH. Irrespective of Ru particle sizes, 1:1 ratio of CH_4 and CO_2 was formed at the initial stage, indicating the absence of complete reforming with water. At the later stage, unfavorable methanation of CO_2 by H_2 was observed over larger Ru particle catalysts, which was suppressed completely over smaller Ru particle catalysts. Accordingly, once CH_4 is formed, it is rather difficult to reform it into H_2 and CO_2 at lower temperatures. However, it might be possible to reform acetic acid with H_2O into H_2 and CO_2. Actually, when we started from AcOH, we were able to achieve the

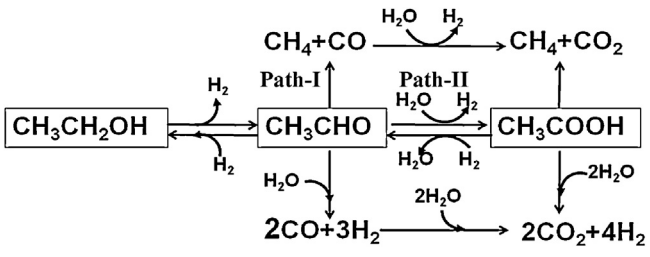

Fig. 7. Reaction scheme.

complete reforming reaction to form H_2 and CO_2, especially over 0.5 wt% Ru/TiO_2 catalysts.

To investigate the relation between EtOH–H_2O and AcOH–H_2O reactions more deeply, we compared the time courses of 1 vol% EtOH + 1 vol% AcOH reaction with 1 vol% EtOH alone reaction over 0.5 wt% Ru/TiO_2 at 473 K. Estimated TOF of the initial rates are summarized in the last two columns in Table 2. The features of time courses of the two reactions are almost identical, indicating strong suppression of AcOH reforming reaction while EtOH is present in the aqueous solution, which is regarded as one reason why achieving direct reforming from EtOH in the aqueous phase is so difficult.

4. Conclusions

Over Ru/TiO_2, aqueous EtOH reforming proceeded through AcH and AcOH. A reversible equilibration process between them (reaction path-II) was identified, where smaller Ru metals exhibited larger TOF than larger Ru metals. Decomposition processes from AcH and AcOH occurred, which formed 1:1 ratio CH_4 and CO (or CO_2) (reaction path-I), and larger Ru metals exhibited larger TOF than smaller metals.

Active sites for reaction path-I was zero-valent larger Ru metal catalysts, whereas positively charged ($Ru^{\delta+}$) smaller Ru would be the active sites for reaction path-II, where CO_2 methanation was inhibited completely. From AcH and AcOH, a certain extent of complete reforming process to form H_2 and CO_2 were observed, especially over smaller Ru metal catalysts.

Inhibition of AcOH reforming was observed while EtOH was present in the solution.

Acknowledgment

The authors are grateful for financial support through the Science Frontier Project from the Ministry of Education Science, Culture, Sports and Technology of Japan.

References

[1] A. Haryanto, S. Fernando, N. Murali, S. Adhikari, Energy Fuels 19 (2005) 2098.
[2] M. Ni, D.Y.C. Leung, M.K.H. Leung, International Journal of Hydrogen Energy 32 (2007) 3238.
[3] G. Jacobs, R.A. Keogh, B.H. Davis, Journal of Catalysis 245 (2007) 326.
[4] F. Can, A. Le Valant, N. Bion, F. Epron, D. Duprez, Journal of Physical Chemistry C 112 (2008) 14145.
[5] Z. Zhong, H. Ang, C. Choong, L. Chen, L. Huang, Physical Chemistry Chemical Physics 11 (2009) 872.
[6] I.O. Cruz, N.F.P. Ribeiro, D.A.G. Aranda, M.M.V.M. Souza, Catalysis Communications 9 (2008) 2606.
[7] Z. Tang, J. Monroe, J. Dong, T. Nenoff, D. Weinkauf, Industrial and Engineering Chemistry Research 48 (2009) 2728.
[8] B. Roy, K. Loganathan, H.N. Pham, A.K. Datye, C.A. Leclerc, International Journal of Hydrogen Energy 35 (2010) 11700.
[9] A.V. Tokarev, A.V. Kirilin, E.V. Murzina, K. Eranen, L.M. Kustov, International Journal of Hydrogen Energy 35 (2010) 12642.
[10] H. Igarashi, T. Fujino, M. Watanabe, Physical Chemistry Chemical Physics 3 (2001) 306–314.
[11] M. Watanabe, T. Suzuki, S. Motoo, Denki Kagaku 40 (1972) 210–211.
[12] R.D. Cortight, R.R. Davda, J.A. Dumesic, Nature 418 (2002) 964.
[13] J.W. Shabaker, R.R. Davda, G.W. Huber, R.D. Cortright, J.A. Dumesic, Journal of Catalysis 215 (2003) 344.
[14] J.W. Shabaker, G.W. Huber, J.A. Dumesic, Journal of Catalysis 222 (2004) 180.

[15] J.W. Shabaker, J.A. Dumesic, Industrial and Engineering Chemistry Research 43 (2004) 3105.
[16] X. Chu, J. Liu, B. Sun, R. Dai, Y. Pei, M. Qiao, K. Fan, Journal of Molecular Catalysis A: Chemical 335 (2011) 129.
[17] T. Rittonen, E. Toukoniitty, D.K. Madnani, A.-R. Leino, K. Kordas, M. Szabo, A. Sapi, K. Arve, J. Warna, J.-P. Mikkola, Catalysis 2 (2012) 68.
[18] P. Yaseneva, S. Pavlova, V. Sadykov, G. Alikina, A. Lykashevich, V. Rogov, S. Belochapkine, J. Ross, Catalysis Today 137 (2008) 23.
[19] A.J. Byrd, K.K. Pant, R.B. Gupta, Fuel 87 (2008) 2956.
[20] R. Trane, S. Dahl, M.S. S-Rasmussen, A.D. Jensen, International Journal of Hydrogen Energy 37 (2012) 6447.
[21] W. Cheng Chiu, R. Fang Hong, H. Ming Chou, International Journal of Hydrogen Energy 38 (2013) 2760.
[22] P.-Y. Sheng, A. Yee, A. Bowmaker, H. Idriss, Journal of Catalysis 208 (2002) 393.
[23] B. Roy, U. Martine, K. Loganathan, A.K. Datye, C.A. Leclerc, International Journal of Hydrogen Energy 37 (2012) 8143.
[24] B. Roy, K. Artyushkova, H.N. Pham, L. Li, A.K. Datye, C.A. Leclerc, International Journal of Hydrogen Energy 37 (2012) 18815.
[25] T. Takanabe, K. Aika, K. Seshen, L. Lefferts, Journal of Catalysis 227 (2004) 101.
[26] A.C. Basagiannis, X.E. Verykios, International Journal of Hydrogen Energy 32 (2007) 3343.
[27] A.C. Basagiannis, X.E. Verykios, Applied Catalysis B: Environmental 82 (2008) 77.
[28] S. Thaicharoensutcharittham, V. Meeyoo, B. Kitiyanan, P. Rangsunvigit, T. Rirksomboon, Catalysis Today 164 (2011) 257.
[29] N. Iwasa, T. Yamane, M. Arai, International Journal of Hydrogen Energy 36 (2011) 5904.
[30] H. Wan, R.V. Chaudhari, B. Subramaniam, Energy Fuels 27 (2013) 487.
[31] Unpublished results.
[32] T. Komaya, A.T. Bell, Z. Weng-Sieh, R. Gronsky, F. Engelke, T.S. King, M. Pruski, Journal of Catalysis 149 (1994) 142.
[33] A.A. Davydov, A.T. Bell, Journal of Catalysis 49 (1977) 332.
[34] F. Solymosi, J.R. Rasko, Journal of Catalysis 15 (1989) 107.
[35] R.L. Martins, M.A.S. Baldanza, M.T. Lima, M. Schmal, Studies in Surface Science and Catalysis 138 (2001) 299.